Nuclear Instruments and Methods in Physics Research A 732 (2013) 577–580

Contents lists available at ScienceDirect

Nuclear Instruments and Methods in Physics Research A

journal homepage: www.elsevier.com/locate/nima

Combining endoscopic ultrasound with Time-Of-Flight PET: The EndoTOFPET-US Project

Benjamin Frisch

CERN, Geneva, Switzerland

On behalf of the EndoTOFPET-US Collaboration

ARTICLE INFO

Available online 15 May 2013

Keywords:
Prostate cancer
Pancreas cancer
PET
Ultrasound
Multimodality
Endoscope

ABSTRACT

The EndoTOFPET-US collaboration develops a multimodal imaging technique for endoscopic exams of the pancreas or the prostate. It combines the benefits of high resolution metabolic imaging with Time-Of-Flight Positron Emission Tomography (TOF PET) and anatomical imaging with ultrasound (US). EndoTOFPET-US consists of a PET head extension for a commercial US endoscope and a PET plate outside the body in coincidence with the head. The high level of miniaturization and integration creates challenges in fields such as scintillating crystals, ultra-fast photo-detection, highly integrated electronics, system integration and image reconstruction. Amongst the developments, fast scintillators as well as fast and compact digital SiPMs with single SPAD readout are used to obtain the best coincidence time resolution (CTR). Highly integrated ASICs and DAQ electronics contribute to the timing performances of EndoTOFPET. In view of the targeted resolution of around 1 mm in the reconstructed image, we present a prototype detector system with a CTR better than 240 ps FWHM. We discuss the challenges in simulating such a system and introduce reconstruction algorithms based on graphics processing units (GPU).

1. Introduction

Pancreas cancer is among the deadliest cancers. Since it is practically symptom-free during its early stages, it often already spread to other organs when it is discovered, leading to 5-year survival rates lower than 2% [1]. It is usually diagnosed with computer tomography (CT), ultrasound (US) being used for staging of the disease. On the other hand, prostate cancer is among the most frequently diagnosed cancer in males, with a life-time risk of 1–6 [1]. US and magnetic resonance tomography (MRI) are the standard imaging procedures.

Both diseases require advanced imaging techniques for their diagnosis and staging. The EndoTOFPET-US collaboration [2] aims at the development and exploitation of a tool for studies of biomarkers specific to pancreas and prostate cancer [3,4]. It conducts research on future radio-labeled tracers that can be used for the diagnosis of these diseases. It also develops a multimodal imaging technique for examination of these organs that combines the benefits of high resolution metabolic information from Time-Of-Flight (TOF) Positron Emission Tomography (PET) and anatomical information from ultrasound (US). EndoTOFPET-US is an international collaboration with 13 partners that includes

- *academic partners*: CERN, Geneva, CH; DESY, Hamburg, DE; the Laboratory of Instrumentation and Experimental Particles Physics, Lisbon, PT; the Technical University Delft, Delft, NL; the Technical University Munich, Munich, DE; the University of Heidelberg, Heidelberg, DE; the University of Milano-Biccoca, Milano, IT.
- *industrial partners*: KLOE, Montpellier, FR; Fibercryst, Lyon, FR; Surgiceye, Munich, DE
- *clinical partners*: University Aix-Marseille, Marseille, FR; Klinikum Rechts der Isar—TU Munich, Munich, DE and University of Lausanne, Lausanne, CH.

EndoTOFPET-US requires the development of two novel detectors, a PET head extension for a commercial US endoscope and a PET plate outside the body in coincidence with the PET head (Fig. 1). Since the pancreas is close to the liver and the heart and the prostate close to the bladder, both are surrounded by organs that have a high uptake of radio-labeled tracers. Good TOF information, obtained with detectors whose coincidence time resolution (CTR) is 200 ps FWHM, should contribute to rejecting background coincidences and reduce the amount of noise in the reconstructed image. 200 ps FWHM correspond to an interval of around 3 cm around the point of emission, sufficient to remove coincidence events outside the organs of interest. EndoTOFPET-US

E-mail address: benjamin.frisch@cern.ch

0168-9002/$ - see front matter © 2013 Elsevier B.V. All rights reserved.
http://dx.doi.org/10.1016/j.nima.2013.05.027

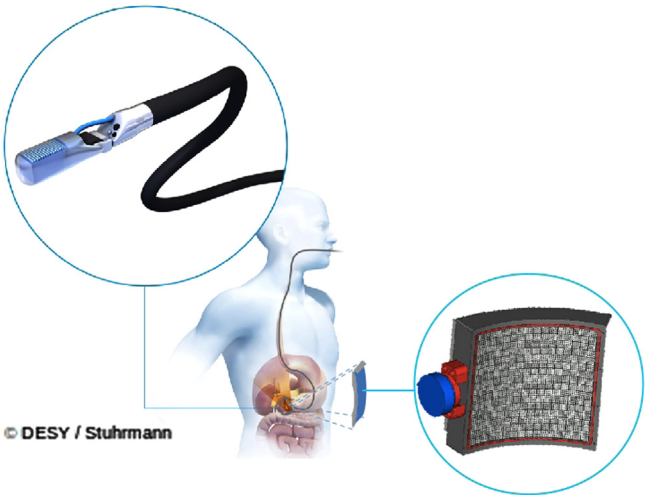

Fig. 1. The EndoTOFPET-US multimodal imaging device, as it would be used for an exam of the pancreas. The top left shows a zoom on the endoscopic probe, with the PET detector attached to the US probe, the lower right shows a zoom on the external detector plate. (©DESY/Stuhrmann)

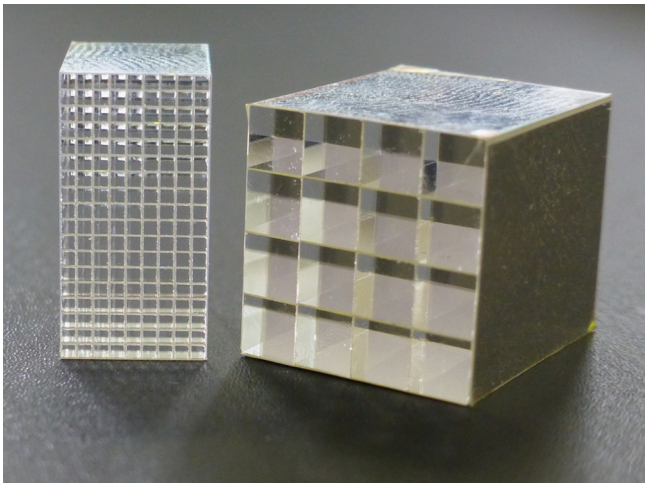

Fig. 2. A side-by-side on-scale photography of a matrix of 9×18 crystals used in the endoscope and a matrix of 4×4 crystals used in the external plate.

shall produce PET images with very high spatial resolution around 1 mm to allow the precise identification of cancerous lesions.

The high level of miniaturization and integration needed to create an endoscopic detector and an external plate with a high number of individual detector channels induces challenges in fields such as scintillating crystals, ultra-fast photo-detection, highly integrated electronics, system integration and image reconstruction.

2. Detector

2.1. Endoscopic detector

The endoscopic internal PET probe requires a solution to place up to 324 individual detector channels including the scintillating crystal, an individual photo-detector for the single-sided readout of each crystal as well as the readout electronics into a volume of 23 mm in diameter and at the maximum 40 mm in length. We use LYSO:Ce scintillating crystals with a cross-section of 0.71×0.71 mm^2 and a length of 10–15 mm in a matrix of 9×18 crystals (Fig. 2). The matrix uses an ESR reflector produced by 3 M as a cladding material and to improve the light transport in the crystal. The endoscopic prototype for the pancreas uses one, the prototype for the prostate two of these matrices.

In the endoscopic probe, the photons emitted by the crystal will be detected by a fully digital silicon photomultiplier (d-SiPM). In comparison to classical analog SiPMs (a-SiPM), the individual single photo-avalanche diodes (SPADs) are not connected to a common output that generates an analog sum signal. Instead, each SPAD is read out by an individual counter. The sum of these counters over all SPADs provides the energy measurement. Additionally, the pixels are connected column-wise to TDCs that measure the exact time of arrival of the photons. This guarantees the most precise timing information regardless of potentially high dark-count rates (DCR) due to a low threshold. The d-SiPM has a total of 416 SPADs and records the timing information with 48 TDCs. This provides a fill factor of 57% [5].

The heat generated by the power dissipation of the electronics requires a cooling system. Water at room-temperature flows through cooling pipes installed in the endoscopic detector head. An insulation separates the cooled inner part of the probe from its surface in contact with the patient.

Since the probe will move in the patient to acquire data from different positions, it has to be tracked. In the case of the pancreatic solution, a magnetic tracking system will be used. The prostatic probe will be tracked by a robot fixed to the examination table, the position of the robot itself being determined with an optical tracking system.

2.2. External plate

The external plate uses 256 matrices of 4×4 LYSO:Ce crystals with an individual size of $3.5 \times 3.5 \times 15$ mm^3 (Fig. 2), coupled to commercial arrays of 4×4 discrete a-SiPM MultiPixel Photon Counters (MPPCs) produced by Hamamatsu. They are read out by a dedicated very fast 64-channel ASIC developed in the frame of this project. Asides offering a high level of integration to fit all 4096 channels on a plate of 230×230 mm^2, it shall offer the possibility of tuning the SiPM bias voltage within a linear range of 0.5 V. Its time bin width shall be better than 50 ps, with a small time jitter to obtain best timing performance. The collaboration develops two solutions in parallel: the STiC-ASIC from the university of Heidelberg and the TOFPET-ASIC from LIP.

The position of the external plate is determined with an optical tracking system.

2.3. DAQ

EndoTOFPET-US will use a dedicated PCIexpress (PCIe) card for the data acquisition (DAQ), installed in the same bed-side workstation that also hosts the GPU cards for the image reconstruction. It acquires information from the endoscopic probe over a 400 Mbit/s serial link, at an expected single event rate of 200 kHz. It also acquires information from a total of 8 front-end boards (FEBs) in the external plate. Each FEB hosts eight ASICs as well as a FPGA that takes care of the slow control but also concentrates event data and sends it to the DAQ card. A total of four different 800 MBit/s serial links take care of transmitting data from the FEBs to the DAQ at a single event rate of 40 MHz [6].

As shown in Fig. 3, the FPGA on the DAQ card preselects coincidence events to lower the event rate passed to the DAQ software to 350 kHz. The software then applies time and energy filters and extracts valid coincidences that are forwarded at a maximum rate of 50 kHz to the reconstruction algorithm [6].

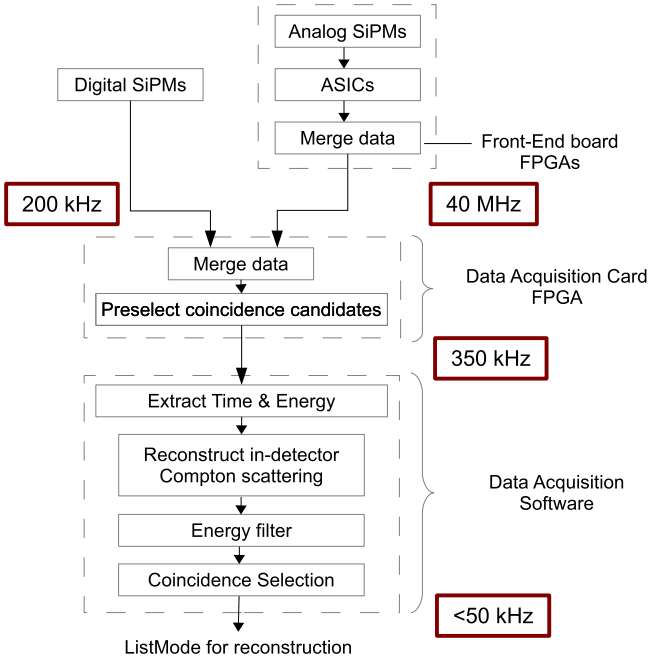

Fig. 3. Schematic summary of the DAQ logic.

2.4. Image reconstruction

The reconstruction needs to master the difficulties that arise from performing a free-hand acquisition with a system that has low sensitivity. First, both detectors can move freely in space: the volume of interest (VOI) cannot be defined in advance as it would be the case in a static PET system. Then, the reconstruction has to deal with a limited-angle problem. Considering the anatomy, the endoscopic probe is very limited in its movement: there will be a lack of information from most angles. In addition, due to the small volume of the endoscopic detector, low sensitivity reduces the amount of available data.

A dedicated algorithm is developed for EndoTOFPET-US [8]. It introduces virtual detector pixels around the VOI and remaps the measured lines-of-response (LORs) into virtual LORs. It then uses a maximum likelihood expectation maximization (MLEM) iterative algorithm to reconstruct the image. The whole image reconstruction process should start as soon as first information is acquired and provide an online feedback to the physician about the data quality and evolution of the image. This will contribute to reduce exam times since the exam can be stopped as soon as sufficient data is acquired. The implementation uses parallelized graphics processing units (GPU) that shall accelerate the reconstruction to a level compatible with the requirements.

3. Characterization

3.1. Scintillating crystals

Prototypes for the external and internal crystal matrices have been ordered. The light emission properties of the matrices have been tested with a reference photomultiplier. Each matrix is placed on this photodetector, irradiated by a ^{137}Cs source and the energy spectrum for the light emitted by all crystals recorded. The photopeak is narrow and confirms the homogeneity of the crystals. It is compatible with the requirement of an energy resolution better than 20%. In dry contact with the photodetector, the light output is around 11,700 photons/MeV; with optical grease, it is around 21,400 photons/MeV. The light output of an external plate matrix in the same conditions is 10,200 photons/MeV in dry contact and 20,400 photons/MeV with optical grease [7].

The timing properties are measured with a-SiPMs similar to the ones planned to be used for the external plate (MPPC 10931-050p, 3×3 mm^3). The measurement uses the time-over-threshold method with the ultrafast amplifier-discriminator chip NINO. The signal is analyzed with a digital oscilloscope LeCroy WR104MXi. The CTR for the combination of an individual $0.71\times0.71\times10$ mm^3 crystal with an individual $3\times3\times15$ mm^3 crystal is 238.0 ± 4.3 ps [7]. A further measurement determines the average CTR for the combination of an individual $0.71\times0.71\times10$ mm^3 crystal with a 4×4 matrix of $3\times3\times15$ mm^3 crystals, connected to a commercial array of 4×4 MPPCs produced by Hamamatsu, to be $\langle CTR\rangle = 249$ ps with a standard deviation of 23 ps [7].

3.2. Digital SiPM

Tests have confirmed the proper operation of a prototype d-SiPM with 4×4 SPADs. If it is operated 2–3 V above breakdown voltage, the DCR can go up to 10 MHz if all SPADs are enabled. Since noisy pixels can selectively be switched off, it is possible to achieve a median DCR of 30-40 kHz at room temperature with 50 % of the pixel population. The single pixel time resolution (SPTR) is measured with blue laser light. If the laser jitter of 35 ps and the clock and PLL jitters of the test board are subtracted, one finds an SPTR of 115 ± 13 ps FWHM [4,5].

3.3. ASIC

Prototypes of both the STiC-ASIC and the TOFPET-ASIC are currently under test. Preliminary results from a 16-channel STiC-ASIC prototype indicate good agreement with the requirements. Its time jitter is less than 30 ps for an input charge of 5 pC. The input bias is linear in a range from 0 V to 0.7 V. Its current power consumption of 19 mW per channel is expected to decrease in the final 64-channel chip [4].

4. Simulation

Simulations of the whole detector system assist the collaboration in their effort to optimize the PET detectors. They are based on GATE, a Geant4 Application for Emission Tomography [9]. Since the latter is not intended to be used with asymmetric geometries, it requires custom extensions. Both the endoscopic detector and the plate are simulated as separate systems in the same simulation run. The exact information about the energy, position and timing of each single hit is stored. An offline digitizer smears this information and creates physically realistic coincidence pairs that are stored in an ASCII list-mode format. A parallel process manager splits the simulation in as many processes as required and schedules them on a multi-core and multi-threaded computer. The movement of the detectors is simulated by varying their position in different processes. A full-body phantom will be implemented in order to provide sufficiently realistic data for the development of the reconstruction algorithm.

Fig. 4a is an image of the implementation of this detector in GATE. It shows the endoscopic probe on the left, the external plate on the right and an arrangement of three sources with an activity of 1 MBq and diameter of 1 mm in a background phantom with an activity concentration 10 times lower than the spherical sources in between. Fig. 4b shows a sagittal slice through two of the point sources in the reconstructed data set. It confirms that this framework is able to simulate and reconstruct phantom geometries. Data has been acquired by rotating the detectors around the

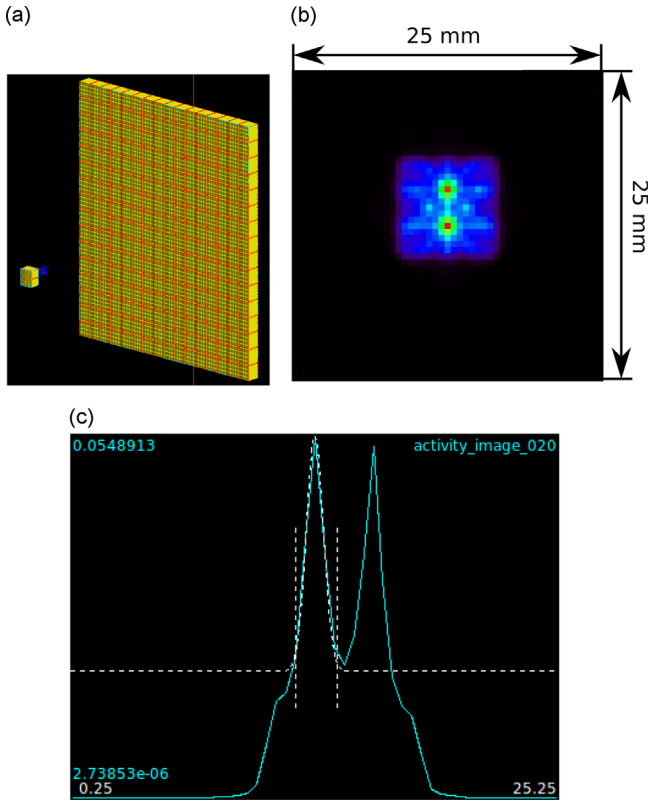

Fig. 4. (a) The prostatic probe and an external plate simulated with three point sources and a background source in GATE, (b) sagittal view of the reconstruction of this simulation and (c) intensity profile through two sources.

phantom and thus circumvents the limited angle problem. Fig. 4c shows the intensity profile through these two sources. It confirms that EndoTOFPET is able to reconstruct a point source with a diameter of 1 mm as a spot with a size of 1.04 mm FWHM.

5. Conclusion

The EndoTOFPET-US collaboration builds a novel multimodal endoscopic ultrasound and PET imaging device. It develops many different technologies in order to achieve this goal. It has designed and received prototypes of all key technologies involved in this project. Preliminary measurements indicate that a CTR of 200 ps is within reach. Simulations confirm that in the ideal case, EndoTOFPET shall be able to achieve an image resolution better than 1 mm. The project now enters its next phase where these technologies are integrated into a full working prototype. This prototype will, in the final phase of this project, enter a clinical trial that proves its use in the diagnosis of pancreas and prostate diseases.

Acknowledgments

The author thanks the collaboration for the privilege of representing it at this conference.

The research leading to these results has received funding from the European Union Seventh Framework Programme (FP7/ 2007-2013) under Grant Agreement n256984. This research is also supported by the Marie-Curie Actions ITN: PicoSEC-MCNeT under Grant Agreement No. 289355.

References

[1] R. Ported, J. Kaplan (Eds.), The Merck Manual for Healthcare Professionals, 18th edition, retrieved March 8th, 2013, at ⟨http://www.merckmanuals.com/professional⟩.
[2] EndoTOFPET-US Proposal: Novel Multimodal Endoscopic Probes for Simultaneous PET/Ultrasound Imaging for Imageguided Interventions, European Union Seventh Framework Program (FP7/2007-2013) under Grant Agreement No. 256984, Health-2010.1.2-1.
[3] T. Meyer, Nuclear Instruments and Methods in Physics Research Section A, in press, http://dx.doi.org/10.1016/j.nima.2012.08.066.
[4] E. Garutti, in: IEEE Nuclear Science Symposium and Medical Imaging Conference Records, 2012, p. 2096.
[5] S. Mandai, E. Charbon, in: IEEE Nuclear Science Symposium and Medical Imaging Conference Records, 2012, p. 1840.
[6] R. Bugalho, et al., Journal of Instrumentation 8 (2012) C02049, http://dx.doi.org/10.1088/1748-0221/8/02/C02049.
[7] E. Auffray, et al. IEEE Nuclear Science Symposium and Medical Imaging Conference Records, 2012, p. 3236.
[8] A. Cserkaszky, et al., GPU-based Monte Carlo for PET image reconstruction: parameter optimization, International Conference on Mathematics and Computational Methods Applied to Nuclear Science and Engineering (M&C 2011), Rio de Janeiro, Brazil, May 8–12, 2011, CD-ROM, Latin American Section (LAS)/American Nuclear Society (ANS), ISBN 978-85-63688-00-2.
[9] S. Jan, et al., Physics in Medicine and Biology 49 (2004) 4543, http://dx.doi.org/10.1088/0031-9155/49/19/007.